STEM CELLS AND DEVELOPMENT
Volume 21, Number 5, 2012

DOI: 10.1089/scd.2011.0160

Effect of In Vitro Passaging on the Stem Cell-Related Properties of Tendon-Derived Stem Cells—Implications in Tissue Engineering

Qi Tan,[1,2,*] Pauline Po Yee Lui,[1–3,*] and Yun Feng Rui[1,2,*]

This study aimed to compare clonogenicity, proliferation, stem cell-related marker expression, senescence, and differentiation potential of rat patellar tendon-derived stem cells (TDSCs) at early (P5), mid (P10), and late (P20, P30) passages. The clonogenicity of the cells was assessed by colony-forming assay and their proliferative potential was assessed by bromodeoxyuridine assay. The surface expression of CD90 and CD73 was assessed by flow cytometry. The cellular senescence was assessed by β-galactosidase activity. The adipogenic, chondrogenic, and osteogenic differentiation potentials of TDSCs were assessed by standard assays after induction. The mRNA expression of tendon-related markers, scleraxis (*Scx*) and tenomodulin (*Tnmd*), was measured by quantitative real-time reverse transcription–polymerase chain reaction. Both the colony numbers and proliferative potential of TDSCs increased with passaging. Concomitantly, there was significant upregulation of β-galactosidase activity with TDSC passaging. The subculture of TDSCs downregulated the expression of CD90 and CD73. Lipid droplets were formed in the early and mid passages of TDSCs upon adipogenic induction, but were absent in the late passages. The expression of peroxisome proliferator activator receptor gamma 2 (*PPARγ2*) and CCAAT/enhancer binding protein alpha (*C/EBPα*) in TDSCs after adipogenic induction decreased with passaging. Chondrogenesis, proteoglycan deposition, collagen type II protein expression, collagen type 2A1 (*Col2A1*), and aggrecan (*Acan*) mRNA expression were less in pellets formed with later passages of TDSCs after chondrogenic induction. The expression of *Scx* and *Tnmd* was lower in the late, compared with early and mid, passages of TDSCs. However, matrix mineralization and expression of alkaline phosphatase (*Alpl*) and osteocalcin (*Bglap*) mRNA after osteogenic induction increased with TDSC passaging. Researchers and clinicians should consider the changes of stem cell-related properties of TDSCs when multiplying them in vitro for tissue engineering.

Introduction

Adult mesenchymal stem cells (MSCs), with their ability for self-renewal and multilineage differentiation potential, are attracting strong attention in regenerative medicine for the repair and replacement of damaged tissues and organs. MSCs were initially identified in bone marrow but later have also been isolated from other tissues such as adipose tissue [1], umbilical cord [2], periodontal ligament [3], articular cartilage [4], muscle [5], periosteum [6], and synovium [7]. Recently, MSCs have also been identified in tendons [8–9] and we have shown that tendon-derived stem cells (TDSCs) could promote tendon repair in an acute rat patellar tendon window injury model (unpublished results).

Although MSCs show high cell renewal potential, they are also vulnerable to replicative senescence [10–17]. A previous study has shown that human bone marrow-derived mesenchymal stem cells (hBMSCs) became senescent with prolonged in vitro culture, as indicated by their decreased multilineage differentiation potential, shortening of mean telomere length, and morphologic alterations [13]. There was also significant loss of telomerase activity in MSCs during prolonged culture, which might cause the MSCs to enter the crisis phase [10]. On the other hand, there were also evidences showing that MSCs could escape replicative senescence and transform to malignant cells during extended culture [18–19].

As TDSCs are being investigated for their potential therapeutic use for the treatment of musculoskeletal disorders, it

[1]Department of Orthopaedics and Traumatology, The Chinese University of Hong Kong, Hong Kong SAR, China.
[2]The Hong Kong Jockey Club Sports Medicine and Health Sciences Centre, The Chinese University of Hong Kong, Hong Kong SAR, China.
[3]Program of Stem Cell and Regeneration, School of Biomedical Science, The Chinese University of Hong Kong, Hong Kong SAR, China.
*All authors have equal contribution in this work.

is important to characterize the biological limitations of these cells with respect to their proliferative and multilineage differentiation potential as they aged during culture in vitro. TDSCs comprised only 1%–2% of total nucleated cells isolated from tendons [9]. The low frequency of TDSCs plus the relative acellularity of tendon therefore necessitates in vitro expansion of TDSCs before clinical use. It is not clear whether the stem cell-related properties of TDSCs can be maintained and how long they can be preserved during in vitro expansion. This study therefore aimed to evaluate the stem cell-related properties, including clonogenicity, proliferative potential, stem cell-related surface marker expression, cellular senescence, and differentiation potential of TDSCs during protracted culture in vitro.

Materials and Methods

Isolation and culture of rat TDSCs

All experiments were approved by the Animal Research Ethics Committee, the Chinese University of Hong Kong. Green fluorescent protein (GFP) Sprague-Dawley rats [SD-Tg (CAG-EGFP) Cz-004Osb, male, 4–6 weeks, body weight of 150–220 g] were used in this study. The procedures for the isolation of TDSCs have been established [9,20]. Briefly, the midsubstance of patellar tendons was excised from healthy rats overdosed with 2.5% sodium phenobarbital. Care was taken that only the midsubstance of patellar tendon tissue, but not the tissue in the bone–tendon junction, was collected. Peritendinous connective tissue was carefully removed and the samples were stored in sterile phosphate-buffered saline (PBS). The tissues were minced, digested with type I collagenase (3 mg/mL; Sigma-Aldrich), and passed through a 70-μm cell strainer (Becton Dickinson) to yield single-cell suspension. The released cells were washed in PBS and resuspended in low-glucose Dulbecco's modified Eagle's medium (LG-DMEM; Gibco) containing 10% fetal bovine serum (FBS), 100 U/mL penicillin, 100 μg/mL streptomycin, and 2 mM L-glutamine (complete culture medium; all from Invitrogen corporation). The isolated nucleated cells were plated at the optimized low density (500 cells/cm^2) for the isolation of stem cells and cultured at 37°C under 5% CO_2 to form colonies. The optimal initial seeding density for TDSC isolation was determined using the colony-forming assay based on the following criteria: (1) the colony size was not affected by colony-to-colony contact inhibition (colonies that were <2 mm in diameter and faintly stained were ignored); and (2) the greatest number of colonies per nucleated cell was obtained. Based on these criteria, the optimal initial cell density thus determined was 500 cells/cm^2 for the isolation of TDSCs from the rat patellar tendon. At day 2 after initial plating, the cells were washed twice with PBS to remove the nonadherent cells. At day 7–10, they were trypsinized and mixed together as passage 0 (P0). TDSCs were subcultured when they reached 80%–90% confluence. Medium was changed every 3 days. The expression of stem cell-related surface markers, clonogenicity, and multilineage differentiation potential of the isolated TDSCs were confirmed by flow cytometry, colony-forming assay, and osteogenic, adipogenic, and chondrogenic differentiation assays as previously described before being used for the experiments in this study [9,20]. Cells at passage 5 (P5), passage 10 (P10), passage 20 (P20), and passage 30 (P30) were used for all experiments. TDSCs from GFP rats were used, because we would trace the fate of these cells in future tissue engineering studies. There is no evidence that the expression of GFP would materially change the biological characteristics of the cells, other than providing a label for cell tracing.

The clonogenicity, proliferation, and stem cell-related surface marker expression of TDSCs at early (P5), mid (P10), and late (P20 and P30) passages were evaluated by colony-forming assay, bromodeoxyuridine (BrdU) cell proliferation assay, and flow cytometry, respectively. The multilineage differentiation potential of TDSCs at different passages were evaluated by adipogenic, chondrogenic, and osteogenic differentiation assays, respectively. The expression of tenogenic markers, scleraxis (*Scx*) and tenomodulin (*Tnmd*), was also investigated. The cellular senescence-associated increase in β-galactosidase activity was tested. The maximal passages that MSCs can achieve in vitro were reported to be 20–30 [10,11,21], and hence, we followed the culture up to P30.

Colony-forming assay

TDSCs at different passages were plated at 100 cells in a 10-cm^2 dish ($n=5$) and cultured for 7 days. The cells were stained with 0.5% crystal violet (Sigma) for counting the number of cell colonies. Colonies that were <2 mm in diameter and those that were faintly stained were ignored.

Cell proliferation assay

TDSCs at different passages were plated at 4×10^3 cells/cm^2 ($n=5$) in a 96-well plate and incubated at 37°C under 5% CO_2. At day 5, cell proliferation was assessed using BrdU assay kit (Roche Applied Science) according to the manufacturer's instruction. The absorbance at 370–490 nm was measured and reported.

Fluorescence-activated cell sorting analysis

For the study of the expression of CD90 in TDSCs at different passages, TDSCs (5×10^5) at different passages were incubated with 1 μg of phycoerythrin (PE)-conjugated mouse anti-rat CD90 monoclonal antibodies (Abcam) or PE-conjugated isotype-matched IgG1 (BD Biosciences) for 1 h at 4°C. For the study of the expression of CD73 in different passages of TDSCs, TDSCs (1×10^6) in different passages were incubated with 1 μg of unconjugated mouse anti-CD73 monoclonal antibodies (BD Biosciences) for 1 h at 4°C, followed by incubation with 1 μg allophycocyanin (APC)-conjugated rat anti-mouse secondary antibodies (BD Biosciences) for 1 h at 4°C. TDSCs incubated with APC-conjugated rat anti-mouse secondary antibodies only were used as negative controls. After washing with PBS and centrifugation at 400 *g* for 5 min, the stained cells were resuspended in 500 μL of ice-cold PBS (with 10% FBS and 1% sodium azide) and subjected to fluorescence-activated cell sorting analysis (BD Biosciences). About 10^4 events were counted for each sample. The percentage of cells with positive signal and the mean geometric fluorescence value of the positive population were calculated using the WinMDI Version 2.9 program (The Scripps Research Institute).

Senescence-associated β-galactosidase activity assay

TDSCs in different passages were plated at 4×10^3 cells/cm^2 ($n=6$) in a 6-well plate and incubated at 37°C under 5% CO_2. At day 5, senescence-associated β-galactosidase activity was assessed by mammalian β-galactosidase assay kit (Thermo Scientific, Inc.) according to the manufacturer's instruction. The absorbance at 405 nm was measured and reported.

Adipogenic differentiation assay

TDSCs in different passages were plated at 4×10^3 cells/cm^2 in a 6-well plate and cultured in complete culture medium until the cells reached confluence. Afterward, the medium was replaced with complete basal medium or adipogenic medium, which was complete basal medium supplemented with 500 nM dexamethasone, 0.5 mM isobutylmethylxanthine, 50 μM indomethacin, and 10 μg/mL insulin (all from Sigma-Aldrich). The cells were cultured for 21 days for the assessment of the presence of oil droplets by Oil Red-O staining ($n=3$) and mRNA expression of adipogenic markers including CCAAT/enhancer binding protein alpha (*C/EBPα*) and peroxisome proliferator activator receptor gamma 2 (*PPARγ2*) by real-time quantitative reverse transcription–polymerase chain reaction (qRT-PCR; $n=6$) [9]. The presence of oil droplets was confirmed by staining the cells with 0.3% fresh Oil Red-O solution (Sigma-Aldrich) for 2 h after fixation with 70% ethanol for 10 min.

Chondrogenic differentiation assay

A pellet culture system was used [9]. About 8×10^5 cells in different passages were pelleted into a micromass by centrifugation at 450 *g* for 10 min in a 15-mL conical polypropylene tube and cultured in complete basal medium or chondrogenic medium at 37°C under 5% CO_2, which contained LG-DMEM (Gibco, Invitrogen Corporation), supplemented with 10 ng/mL transforming growth factor-β3 (R&D Systems), 500 ng/mL bone morphogenetic protein-2 (R&D Systems), 10^{-7} M dexamethasone, 50 μg/mL ascorbate-2-phosphate, 40 μg/mL proline, 100 μg/mL pyruvate (all from Sigma-Aldrich), and 1:100 diluted BD™-ITS + universal culture supplement Premix (6.25 mg/mL insulin, 6.25 mg/mL transferrin, 6.25 mg/mL selenous acid, 1.25 mg/mL bovine serum albumin (BSA), and 5.35 mg/mL linoleic acid; Becton Dickinson). At day 21, the pellet was fixed for hematoxylin and eosin (H&E) staining, safrainin-O (SO)/fast green staining, and immunohistochemical staining of collagen type II ($n=3$). The mRNA expression of collagen type 2A1 (*Col2A1*) and aggrecan (*Acan*) was also assessed at day 21 by qRT-PCR, as described later ($n=6$).

Histological analysis of cell pellet. The cell pellet was fixed in 4% paraformaldehyde, dehydrated, and embedded in paraffin. Sections were cut at a thickness of 5 μm, stained with H&E or SO/fast green after deparaffination [9], and viewed using a LEICA Q500MC microscope (Leica Cambridge Ltd.).

Immunohistochemical staining. Immunohistochemical staining was performed as previously described [9]. Briefly, paraffin-embedded sections were deparaffinized in xylene and dehydrated through graded alcohol. Endogenous peroxidase activity was quenched with 3% hydrogen peroxide for 20 min at room temperature. Antigen retrieval was then performed with 2 mg/mL protease (Calbiochem, Bie and Berntsen) at 37°C for 30 min for collagen type II detection. Residual enzymatic activity was removed by washing the sections with PBS. After blocking the sections with 5% goat serum for 20 min at room temperature, the sections were incubated with mouse monoclonal antibody against rat collagen type II (Neomarkers-Biogen, Lab Vision; 1:100 dilution with 5% goat serum in PBS containing 1% BSA) overnight at 4°C. The spatial localization of collagen type II was visualized by incubating the sections with goat anti-mouse IgG horseradish peroxidase-conjugated secondary antibody (Chemicon International) for an hour at room temperature, followed by incubating the sections with 3,3′-diaminobenzidine tetrahydrochloride (DAKO) in the presence of H_2O_2. Afterward, the sections were rinsed, counterstained with hematoxylin, dehydrated with graded ethanol and xylene, and mounted with DPX. Primary antibody was replaced with blocking solution in the sections that served as negative control. Articular cartilage of femora condyle was used as positive control. The sections were examined under light microscopy (Leica DMRXA2; Leica Microsystems Wetzlar GmbH).

Osteogenic differentiation assay

TDSCs in different passages were plated at 4×10^3 cells/cm^2 in a 6-well plate and cultured in complete culture medium until the cells reached confluence. They were then incubated in complete basal medium or osteogenic medium, which was complete basal medium supplemented with 1 nM dexamethasone, 50 mM ascorbic acid, and 20 mM β-glycerolphosphate (all from Sigma-Aldrich) for 14 and 21 days for the assessment of mineralized nodule formation by Alizarin Red S staining. The mRNA expression of osteogenic markers including alkaline phosphatase (*Alpl*) and osteocalcin (*Bglap*) were also assessed on day 14 by qRT-PCR ($n=6$) [9,20]. For the Alizarin Red S staining assay, the cell/matrix layer was washed with PBS, fixed with 70% ethanol, and stained with 0.5% Alizarin Red S (pH 4.1; Sigma). To quantify the amount of Alizarin Red S bound to the mineralized nodules, the acetic acid extraction method was used according to a previous report [22]. In brief, 1 mL of 10% (v/v) acetic acid was added to each well at room temperature for 30 min. The cell monolayer was scraped off the plate with a cell scraper and transferred to a 1.5-mL microcentrifuge tube. After vortexing for 30 s, the mixture was overlaid with 1.25 mL mineral oil, heated to exactly 85°C for 10 min, and cooled on ice for 5 min. The mixture was then centrifuged at 20,000 *g* for 15 min. Five-hundred microliters of the supernatant was transferred to a new 1.5-mL microcentrifuge tube and neutralized with 200 μL of 10% (v/v) ammonium hydroxide. The color intensity of 150 μL of the solution was measured in triplicate at an optical density of 405 nm in a 96-well plate.

Quantitative real-time reverse transcription–polymerase chain reaction

qRT-PCR was performed as previously described [23]. Cells were harvested and homogenized for RNA extraction with Rneasy mini kit (Qiagen). The mRNA was reverse-transcribed to cDNA by the First Strand cDNA kit

(Promega). About 5 μL of total cDNA of each sample was amplified in final volume of 25 μL of reaction mixture containing Platinum® SYBR® Green qPCR SuperMix-UDG ready-to-use reaction cocktail and specific primers for *C/EBPα*, *PPARγ2*, *Col2A1*, *Acan*, *Scx*, *Tnmd*, *Alpl*, *Bglap*, or *β-actin* using the ABI StepOne Plus system (all from Applied Biosystems; Table 1). Cycling conditions were denaturation at 95°C for 10 min, 45 cycles at 95°C for 20 s, optimal annealing temperature (Table 1) for 30 s, 72°C for 30 s, and finally, 60°C–95°C with a heating rate of 0.1°C/s. The expression of target gene was normalized to that of *β-actin* gene. Relative gene expression was calculated using the $2^{-\Delta CT}$ formula.

Data analysis

Results were shown in boxplots. Comparison of stem cell-related properties of TDSCs in different passages was done using the Kruskal–Wallis test followed by post hoc pairwise comparison with Mann–Whitney *U* test. Comparison of gene expression or mineralization in induction and basal media in each passage was done using the Mann–Whitney *U* test. All the data analysis was done using SPSS analysis software (SPSS, Inc.; version 16.0). $P \leq 0.05$ was regarded as statistically significant.

Results

Clonogenicity and proliferative potential

The colony number increased with passaging in vitro (overall $P = 0.004$; Fig. 1a, b). The colony number was significantly higher at P20 and P30 compared with that at P5 (both post hoc $P = 0.009$; Fig. 1b). The colony number at P30 was also significantly higher at P30 compared with that at P10 (post hoc $P = 0.016$; Fig. 1b).

TDSCs at mid (P10) and late (P20, P30) passages proliferated faster than those at the early passage (P5; overall $P = 0.001$; all post hoc $P = 0.009$; Fig. 2). The proliferative potential of TDSCs at P20 (post hoc comparison: $P = 0.016$) and P30 (post hoc comparison: $P = 0.009$) was also significantly higher than that at P10 (Fig. 2).

Stem cell-related surface marker expression

We compared the stem cell-related surface marker expression in TDSCs in different passages. The surface expression of CD90 and CD73 was downregulated during passaging as shown by the decrease in geometric mean fluorescence intensity and percentage of cells showing positive signal from early (P5) to late (P30) passages (Fig. 3).

Senescence-associated β-galactosidase activity assay

The senescence-associated β-galactosidase activity in TDSCs increased with passaging (overall $P < 0.001$; Fig. 4). There was significantly higher β-galactosidase activity in TDSCs at P30, P20, and P10 compared with cells at P5 (post hoc $P = 0.004$, 0.004, and 0.006, respectively; Fig. 4). The β-galactosidase activity in TDSCs at P30 was also higher than cells at P10 and P20 (both post hoc $P = 0.004$; Fig. 4). Higher β-galactosidase activity was also observed in TDSCs at P20 compared with cells at P10 (post hoc $P = 0.024$; Fig. 4).

Adipogenic differentiation potential

No Oil Red O-positive oil droplet was observed in TDSCs in basal medium in all passages tested (Fig. 5a). Oil Red O-positive oil droplets were observed in both early (P5) and mid (P10) passages of TDSCs (Fig. 5a, arrows), but they were lost in the late passages (P20, P30) upon adipogenic induction (Fig. 5a).

Adipogenic induction increased the expression of *PPARγ2* in TDSCs at all passages except at P10, which was marginally insignificant ($P = 0.055$; Fig. 5b). On the other hand, the expression of *C/EBPα* upon adipogenic induction increased only in TDSCs at early (P5: $P = 0.004$) and mid (P10: $P = 0.004$)

Table 1. Primer Sequences and Condition for Quantitative Real-Time Reverse Transcription–Polymerase Chain Reaction

Gene	*Primer nucleotide sequence*	*Product size (bp)*	*Annealing temperature (°C)*	*Accession number*
β-actin	5′-ATC GTG GGC CGC CCT AGG CA-3′ (forward) 5′-TGG CCT TAG GGT TCA GAG GGG-3′ (reverse)	243	52	NM_031144
C/EBPα	5′-AAGGCCAAGAAGTCGGTGGA-3′ (forward) 5′-CAGTTCGCGGCTCAGCTGTT-3′ (reverse)	189	55	NM_012524.2
PPARγ2	5′-CGGCGATCTTGACAGGAAAG-3′ (forward) 5′-GCTTCCACGGATCGAAACTG-3′ (reverse)	174	59	AB019561
Col2A1	5′-ATGACAATCTGGCTCCCAACACTGC-3′ (forward) 5′-GACCGGCCCTATGTCCACACCGAAT-3′ (reverse)	364	55	BT007205
Acan	5′-CTTGGGCAGAAGAAAGATCG-3′ (forward) 5′-GTGCTTGTAGGTGTTGGGGT-3′ (reverse)	158	58	J03485
Tnmd	5′-GTGGTCCCACAAGTGAAGGT-3′ (forward) 5′-GTCTTCCTCGCTTGCTTGTC-3′ (reverse)	60	52	NM_022290.1
Scx	5′-AACACGGCCTTCACTGCGCTG-3′ (forward) 5′-CAGTAGCACGTTGCCCAGGTG-3′ (reverse)	102	58	NM_001130508.1
Alpl	5′-TCCGTGGGTCGGATTCCT-3′ (forward) 5′-GCCGGCCCAAGAGAGAA-3′ (reverse)	85	58	NM_013059.1
Bglap	5′-GAGCTGCCCTGCACTGGGTG-3′ (forward) 5′-TGGCCCCAGACCTCTTCCCG-3′ (reverse)	263	60	M23637

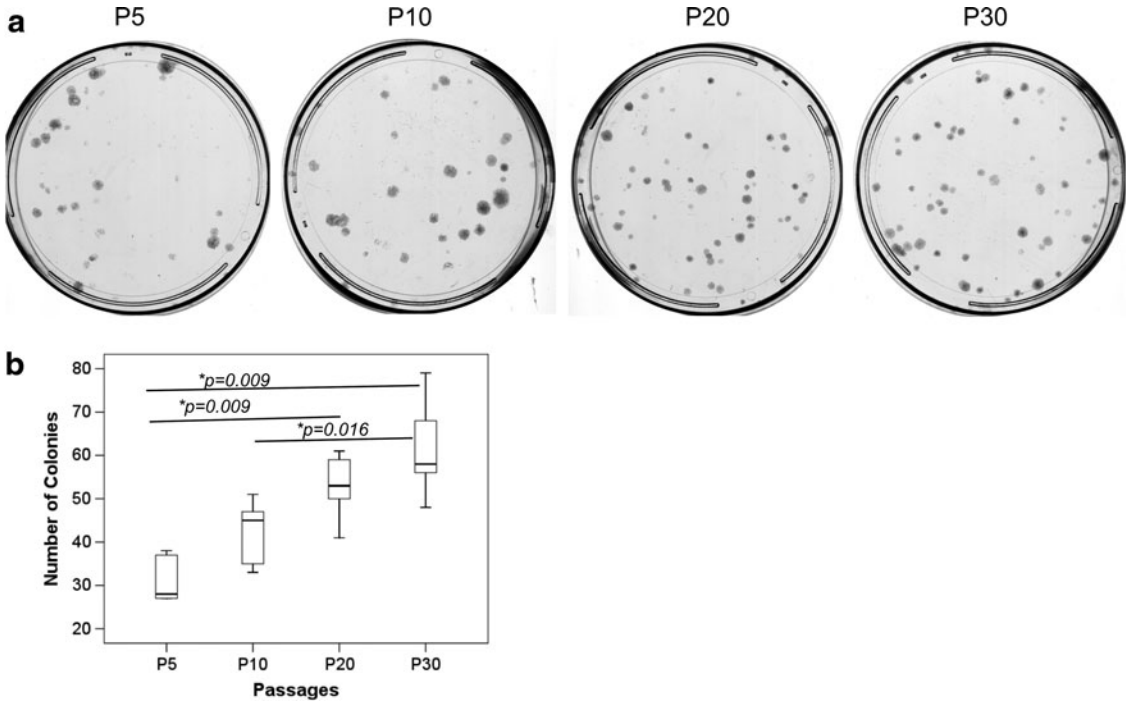

FIG. 1. **(a)** Photomicrographs showing the number of cell colonies in different passages of TDSCs. **(b)** Boxplot showing the number of colonies in different passages of TDSCs. *$P \leq 0.05$ in post hoc comparison of the two groups as indicated by the two ends of the solid line. TDSCs, tendon-derived stem cells.

passages but not for cells at late passages (P20: $P = 0.078$; P30: $P = 0.855$; Fig. 5c).

The mRNA expression of *PPARγ2* and *C/EBPα* in TDSCs significantly decreased with in vitro passaging upon adipogenic induction (*PPARγ2*, overall $P = 0.005$; *C/EBPα*, overall $P = 0.006$; Fig. 5b, c). The expression of *PPARγ2* upon adipogenic induction was significantly higher in early passage (P5) of TDSCs when compared with that in mid (P10) and late (P20, P30) passages of TDSCs (post hoc vs. P5 and P10: $P = 0.004$; P20: $P = 0.004$; P30: $P = 0.037$) as well as in mid passage (P10) of TDSCs when compared with cells in the late passage of P20 (post hoc $P = 0.025$; Fig. 5b). Similarly, the expression of *C/EBPα* in late passage (P20) of TDSCs was significantly lower than that in early (P5) and mid (P10) passages upon adipogenic induction (both post hoc $P = 0.004$; Fig. 5c). The expression of *C/EBPα* in late (P30) passage of TDSCs was also significantly lower than that in cells at early (P5) passage after adipogenic induction (post hoc $P = 0.045$; Fig. 5c). Although there was a statistically significant decrease in the mRNA expression of *PPARγ2* and *C/EBPα* in TDSCs in basal medium with in vitro passaging (*C/EBPα*, overall $P = 0.031$; *PPARγ2*, overall $P = 0.001$), the change was actually very small (Fig. 5b, c).

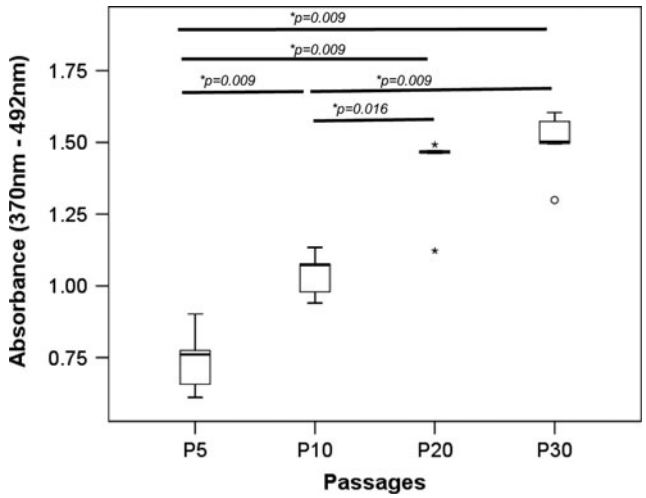

FIG. 2. Boxplot showing the proliferative potential of different passages of TDSCs as indicated by bromodeoxyuridine assay. *$P \leq 0.05$ in post hoc comparison of the two groups as indicated by the two ends of the solid line. *above and below the box of P20 represent extreme values of the data set while "o" below the box of P30 represents outliner of the data set.

Chondrogenic differentiation potential

Cell pellet could be formed only with TDSCs in early passage (P5) in basal medium (Fig. 6a). However, no chondrocyte-like cells were observed in these pellets (Fig. 6a). On the other hand, chondrocyte-like cells could be observed in cell pellets formed by early (P5) and mid (P10) passages of TDSCs upon chondrogenic induction (Fig. 6a, arrows). Less chondrocyte-like cells were observed in cell pellets formed by late passages (P20 and P30) of TDSCs upon chondrogenic induction (Fig. 6a, arrows). Strong deposition of proteoglycan (Fig. 6b) and expression of protein collagen type II (Fig. 6c) were observed in pellets formed by TDSCs in early passage (P5) upon chondrogenic induction. The deposition of proteoglycan and the expression of protein collagen type II decreased sharply in pellets formed by mid passage (P10) of TDSCs and

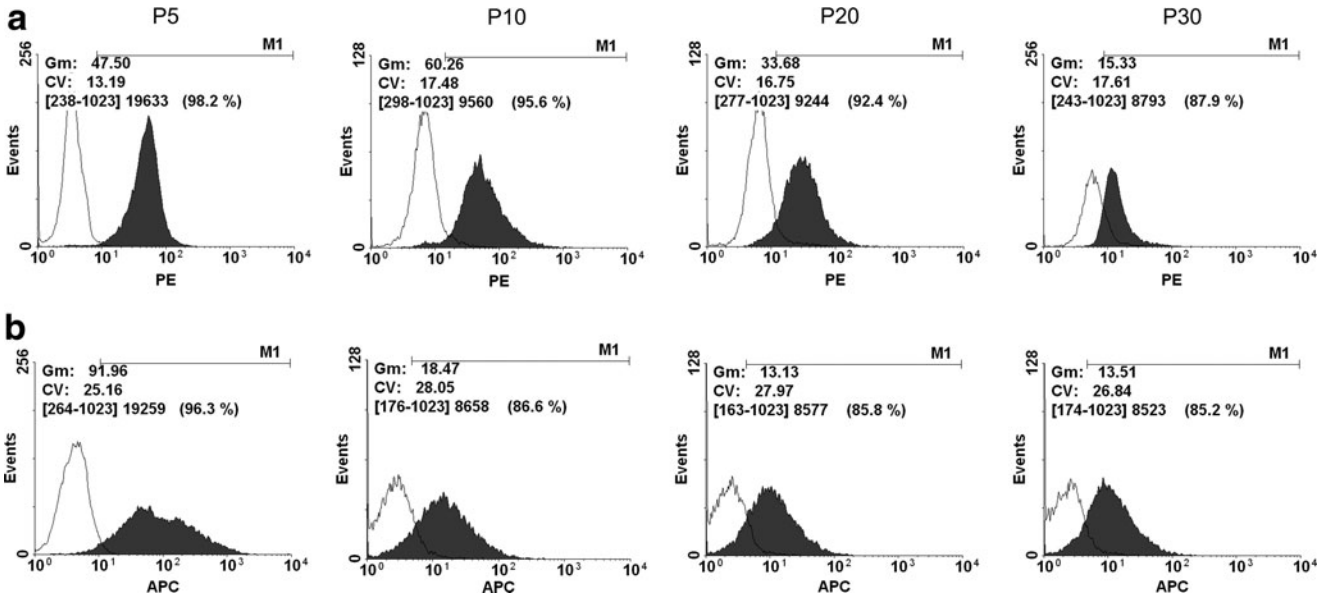

FIG. 3. Histograms showing the expression of **(a)** CD90 and **(b)** CD73 in different passages of TDSCs: Filled area shows the expression of target stem cell markers and open area shows the expression in the corresponding istotype control (PE or APC). Gm, geometric mean fluorescence value of the positive population; Cv, coefficient of variation. The percentage of cells showing positive expression is shown within parentheses. PE, phycoerythrin; APC, allophycocyanin.

became undetectable in pellets formed by late passages (P20 and P30) of TDSCs upon chondrogenic induction (Fig. 6b, c).

The expression of *Col2A1* and *Acan* in TDSCs was significantly higher in chondrogenic compared with that in basal media except in late passages of TDSCs (cells at P20 for *Col2a1* and cells at P30 for *Acan*; Fig. 6d, e). There was significant decrease in the expression of *Col2A1* and *Acan* after chondrogenic induction with passaging (both overall $P < 0.001$; Fig. 6d, e). The expression of *Col2A1* was significantly higher in early passage (P5) compared with that in late passages (P20 and P30) of TDSCs after chondrogenic induction (both post hoc $P = 0.004$; Fig. 6d). The expression of *Col2A1* was also significantly higher in mid passage (P10) compared with that in late passages (P20 and P30) of TDSCs after chondrogenic induction (both post hoc $P = 0.004$; Fig. 6d). There was a significant passage-dependent decrease in the expression of *Acan* in TDSCs except the expression of *Acan* between P5 and P10 after chondrogenic induction (Fig. 6e). We also detected significant change in the expression of *Col2A1* among different passages of TDSCs in the basal medium (overall $P = 0.005$; Fig. 6d). However, the change was very small. There was no significant change in the expression of *Acan* among different passages of TDSCs in the basal medium (overall $P = 0.682$; Fig. 6e).

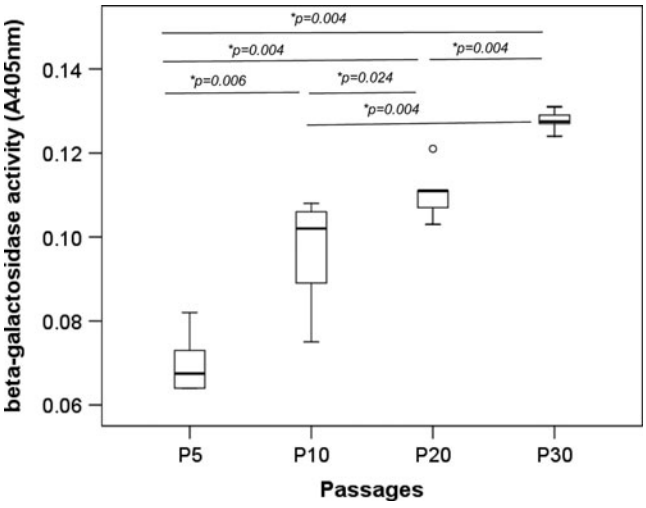

FIG. 4. Boxplot showing the senescence-associated β-galactosidase activity measured at an optical density of 405 nm in different passages of TDSCs. *$P \leq 0.05$ in post hoc comparison of the two groups as indicated by the two ends of the solid line. "o" above the box of P20 represents outliner of the data set.

Tendon-related marker expression

The expression of *Scx* (overall $P = 0.013$; Fig. 7a) and *Tnmd* (overall $P = 0.001$; Fig. 7b) in TDSCs decreased with passaging. The expression of *Scx* in TDSCs remained stable from P5 to P20 but decreased at P30, with significant lower expression in TDSCs at P30 compared with cells at P5 and P10 (both post hoc $P = 0.004$; Fig. 7a). The expression of *Tnmd* was significantly lower in TDSCs at P30 compared with those at P5, P10, and P20 (all post hoc $P = 0.004$; Fig. 7b). The expression of *Tnmd* was also significantly lower in TDSCs at P20 compared with cells in P5 (post hoc $P = 0.016$; Fig. 7b).

Osteogenic differentiation potential

There was significantly higher mineralization of the extracellular matrix, as indicated by Alizarin Red S staining, in TDSCs in osteogenic compared with basal media in all passages tested (all $P = 0.004$; Fig. 8b). Despite the decrease in adipogenic and chondrogenic differentiation potential and tendon-related markers in TDSCs during in vitro subculture, the mineralization of TDSCs increased with passaging upon osteogenic induction (overall $P = 0.001$; Fig. 8a, b). The

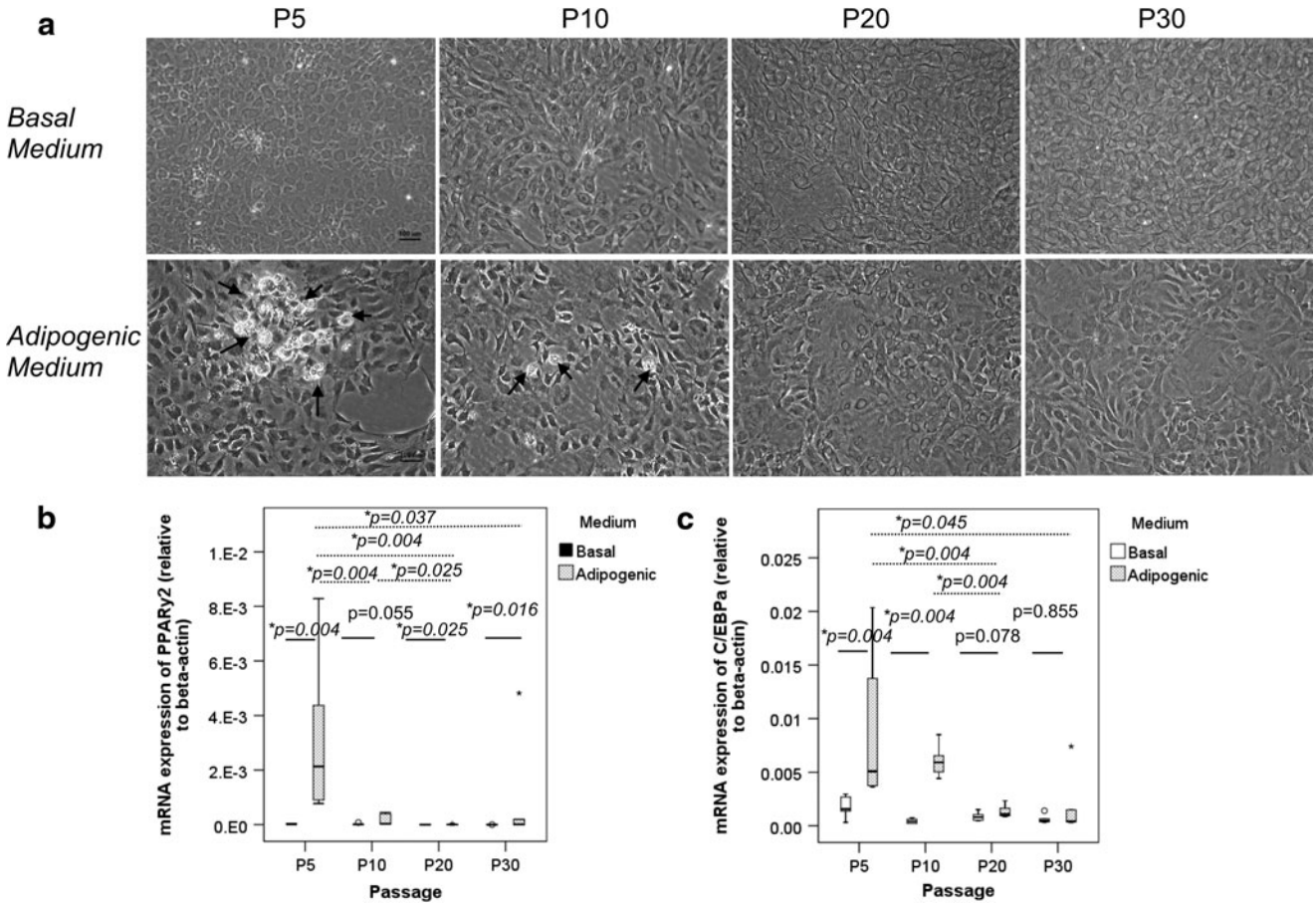

FIG. 5. **(a)** Photomicrographs showing the adipogenic differentiation of different passages of TDSCs in basal or adipogenic media at day 21 as assessed by Oil Red-O staining. Scale bar: 100 μm. *Arrows*: oil droplets. Boxplots showing the mRNA expression of **(b)** *PPARγ2* and **(c)** *C/EBPα* in different passages of TDSCs in basal or adipogenic media. Dotted line: post hoc comparison of two different TDSC passages as indicated by the two ends of the dotted line after adipogenic induction; solid line: comparison between basal and adipogenic media at different TDSC passages; $*P \leq 0.05$; In **(b)** and **(c)**, "o" and "*" above the boxes of P30 represent outliner and extreme value of the data set, respectively.

mineralization was significantly higher in TDSCs at P30 compared with cells in P5, P10, and P20 passages (all post hoc $P = 0.004$) as well as in TDSCs at P20 (post hoc $P = 0.004$) and P10 (post hoc $P = 0.016$) compared with cells at P5 after osteogenic induction for 21 days (Fig. 8b).

The mRNA expression of *Alpl* and *Bglap* significantly increased upon osteogenic induction for 14 days in late passages (P20 and P30) but not in early (P5) and mid (P10) passages of TDSCs (Fig. 8c, d). The expression of *Alpl* and *Bglap* after osteogenic induction increased with in vitro passaging (overall $P < 0.001$ and $P = 0.001$, respectively; Fig. 8c, d). There was a significant passage-dependent increase in the expression of *Alpl* in TDSCs except the expression of *Alpl* between P5 and P10 after osteogenic induction for 14 days (Fig. 8c). The expression of *Bglap* was also significantly higher in late passages (P20 and P30) compared with early (P5) and mid (P10) passages of TDSCs after osteogenic induction for 14 days (all post hoc $P = 0.004$; Fig. 8d). There was significant difference in the expression of *Alpl* in basal medium among different passages of TDSCs (overall $P < 0.001$; all post hoc pairwise comparison: $P = 0.004$). There was no significant difference in the expression of *Bglap* in basal medium among different passages of TDSCs (overall $P = 0.055$).

Discussion

A large number of MSCs are required for therapeutic application of these cells in tissue repair. Therefore, in vitro cell expansion and optimization of culture conditions for large-scale production of MSCs is crucial. The cells have to preserve their stem cell-related properties during the prolonged in vitro passaging. Previous studies have shown that MSCs entered senescence and started losing their stem cell characteristics during in vitro passaging, which affected the application of MSCs for tissue engineering [10–17]. This study aimed to examine the stem cell-related properties of TDSCs during in vitro subculture. This information is useful for in vitro expansion of these cells, not only for the application of these cells for tissue engineering but also for understanding the roles of these cells in tendon physiology and pathology in an in vitro cell culture system.

Both the clonogenicity and proliferative potential of TDSCs increased with passaging. The increase in clonogenicity with in vitro subculture is likely due to the enrichment of stem/progenitor cells with time. The increase in proliferative potential of TDSCs during passing might be hence explained by the increase in the number of stem/progenitor cells, which

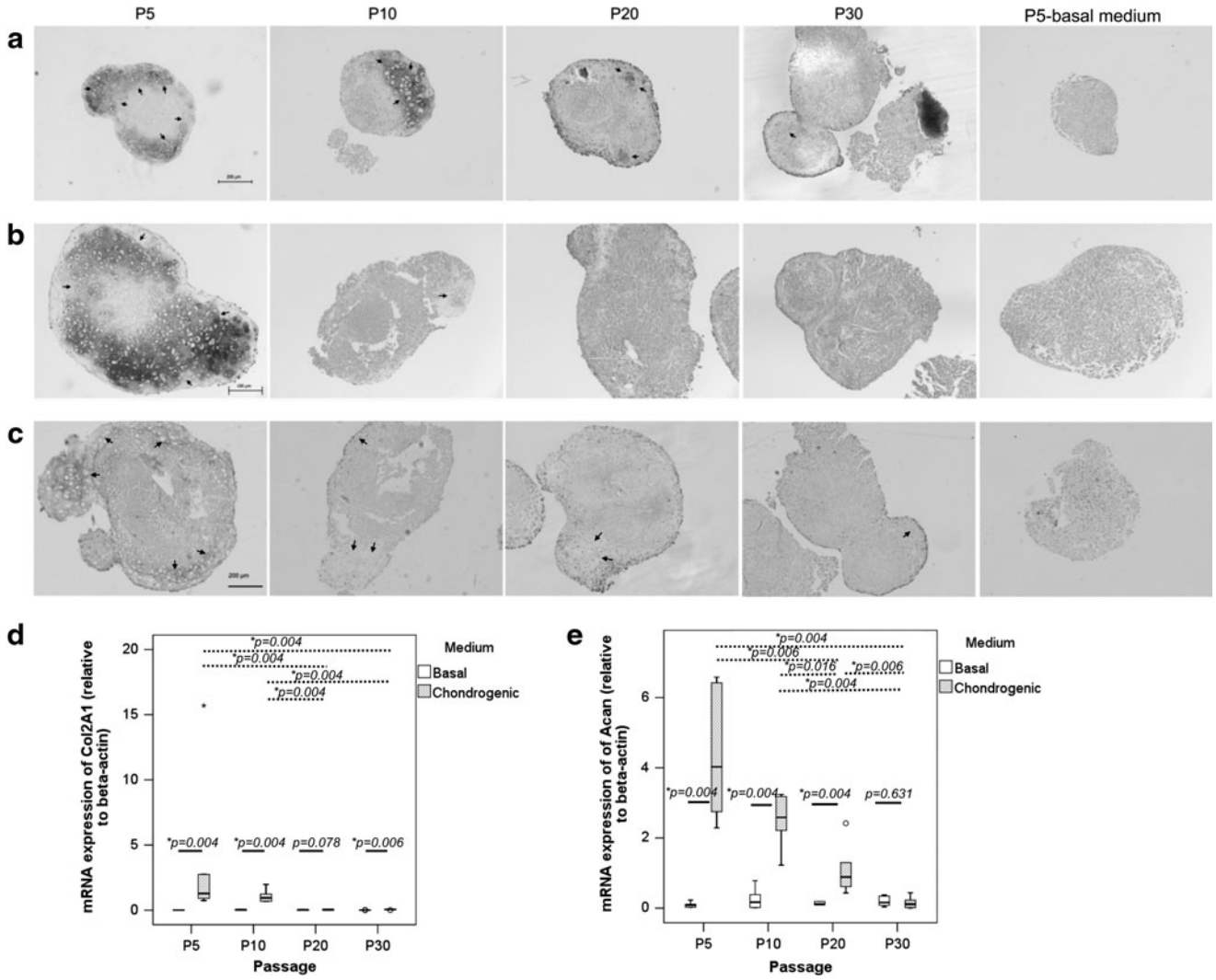

FIG. 6. Photomicrographs showing the chondrogenic differentiation of different passages of TDSCs in chondrogenic medium at day 21 as assessed by **(a)** hematoxylin and eosin staining, **(b)** Safranin O/Fast Green staining, and **(c)** immunohistochemical staining of collagen type II. Scale bar: 200 μm **(a)**, 100 μm **(b)**, and 200 μm **(c)**. *Arrows*: chondrocyte-like cells. Boxplots showing the mRNA expression of **(d)** *Col2A1* and **(e)** *Acan* in different passages of TDSCs in basal or chondrogenic media. Dotted line: post hoc comparison of two different TDSC passages as indicated by the two ends of the dotted line after chondrogenic induction; solid line: comparison between basal and chondrogenic media at different TDSC passages; $*P \leq 0.05$; "*" above the box of P5 in **(d)** and "o" above the box of P20 in **(e)** represent extreme value and outliner of the data set, respectively.

proliferated faster compared with the differentiated cells. Our finding on clonogenicity and proliferative potential of TDSCs during passaging was different from previous studies that reported the contrary [10–11,13–16,24]. Zhang and Wang [24] reported that the population doubling (PD) times of patellar TDSCs and Achilles TDSCs increased at late passages (>12), suggesting senescence of the cells during subculture. Muraglia et al. [14] also reported that hBMSCs grew faster at the primary culture level and they gradually slowed down to reach a complete stop after about 19–23 PDs.

Despite the increase in clonogenicity and cell proliferation, the senescence-associated β-galactosidase activity of TDSCs increased with passaging in this study. The surface expression of CD90 and CD73 in TDSCs was downregulated during passaging through P30 in our study. This was consistent with a previous report showing that markers distinguishing MSCs from fibroblasts were downregulated with passaging [25]. They reported that although the percentage of cells with CD105, CD44, CD90, CD166, HLA-ABC, and HLA-DR expression remained high over passaging, there was a significantly higher percentage of cells with CD9 and lower percentage of cells with CD106, integrin alpha 11, and CD146 in hBMSCs at P6 compared with cells at P2 [25]. However, our findings were different from other studies that reported that the expression of stem cell markers in human and rhesus MSCs isolated from bone marrow and adipose tissue remained stable during extended passages [10]. The expression of CD29, CD44, CD90, and CD166 in adipose tissue-derived MSCs was also reported to remain stable with passaging [26].

In addition, there was loss of adipogenic, chondrogenic, and tenogenic differentiation capacity of the cells with increased commitment of the cells toward the osteogenic lineage during subculture. The progressive loss of multilineage differentiation potential with in vitro passaging was also

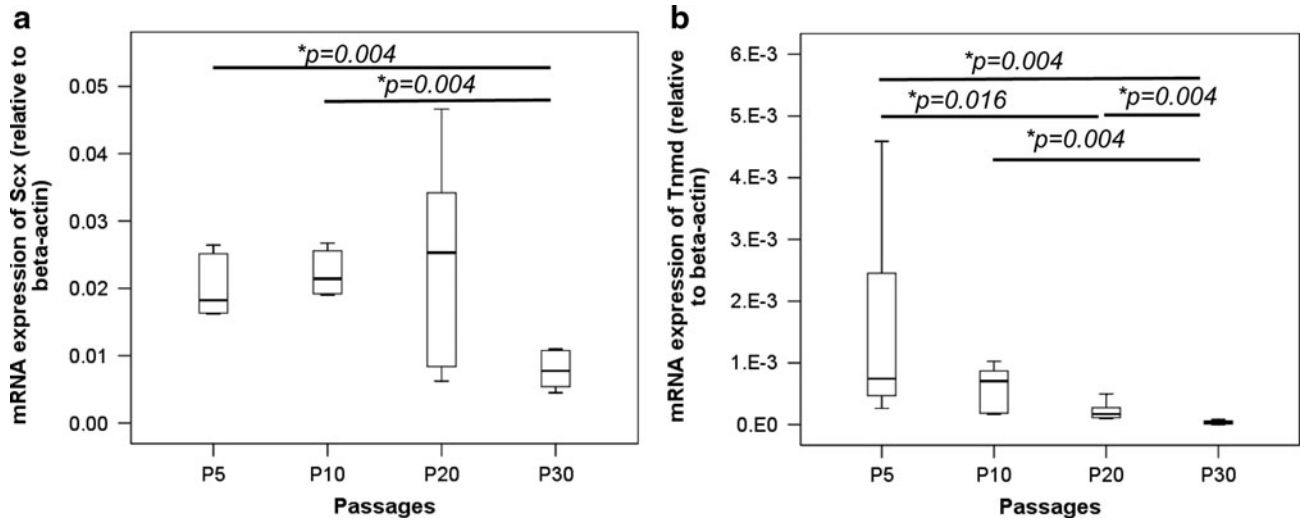

FIG. 7. Boxplots showing the mRNA expression of tendon-related markers, **(a)** *Scx* and **(b)** *Tnmd*, in different passages of TDSCs. $*P \leq 0.05$ in post hoc comparison of the two groups as indicated by the two ends of the solid line.

reported in previous studies [10,13–15,21,27–30]. The alkaline phosphatase activity of rat BMSCs at P1 was almost 5 times that of rat BMSCs at P3 under the osteogenic differentiation condition [28]. Banfi et al. [15] reported that hBMSCs had a markedly diminished proliferation rate up to P5 and gradually lost their multiple differentiation potential up to P4. Their bone-forming efficiency in vivo was reduced by about 36 times at first confluence when compared with fresh bone marrow. Muraglia et al. [14] proposed a hierarchy of the BMSC differentiation pathway, where the adipogenic lineage diverged and became independent earlier, whereas the osteochondrogenic lineages proceeded together, possibly diverging later. The osteogenic pathway may be the "default" lineage that these cells can progress through, possibly

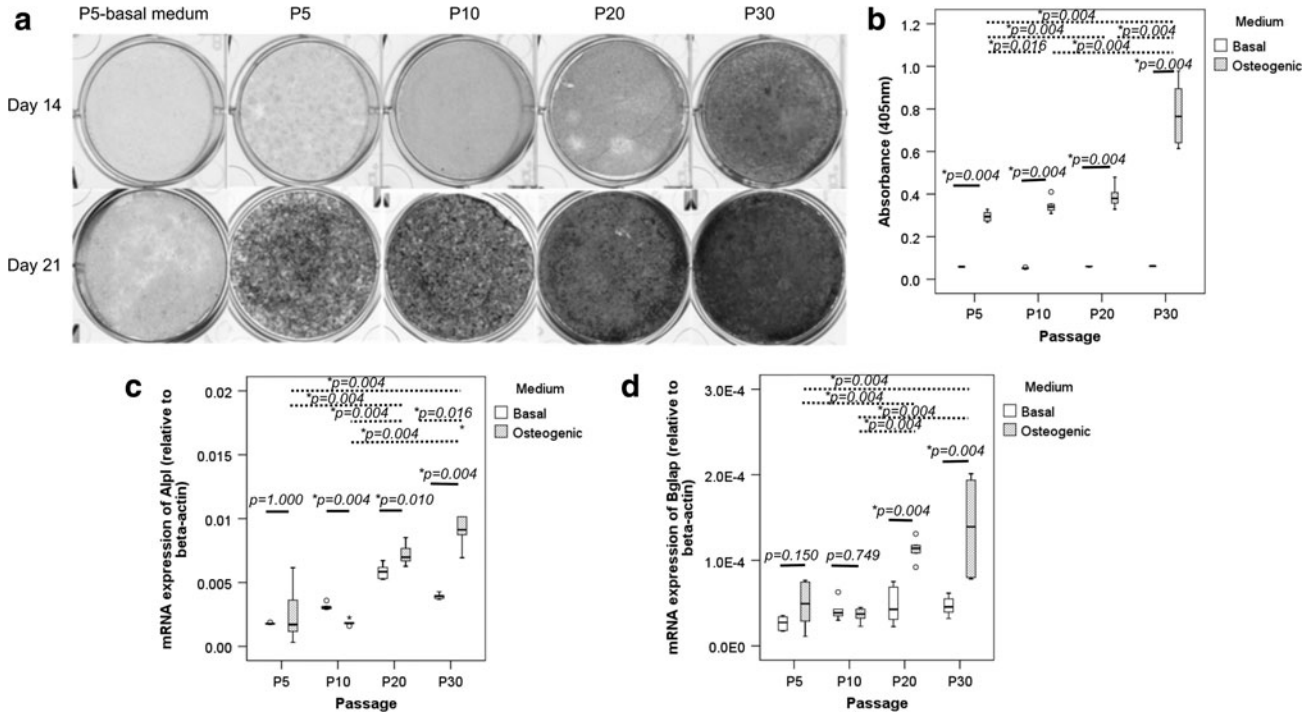

FIG. 8. **(a)** Photomicrographs showing the osteogenic differentiation of different passages of TDSCs in basal (P5 only) or osteogenic media at day 14 or 21 as assessed by Alizarin Red S staining. The darker the gray color, the higher is the intensity of Alizarin Red S staining. **(b)** Boxplot showing the quantitative measurement of Alizarin Red S bound to the mineralized nodules in different passages of TDSCs at day 21. Boxplots showing the mRNA expression of **(c)** *Alpl* and **(d)** *Bglap* in different passages of TDSCs in basal or osteogenic media. Dotted line: post hoc comparison of two different TDSC passages as indicated by the two ends of the dotted line after osteogenic induction; solid line: comparison between basal and osteogenic media at different TDSC passages; $*P \leq 0.05$; "o" and "*" above or below the box represent outliner and extreme value of the data set, respectively.

because of either an intrinsic osteogenic commitment of the cells or an in vitro culture conditions favoring osteogenesis. Similar result was reported by Banfi et al. [15]. They reported that spontaneous osteogenic, but not chondrogenic and adipogenic, differentiation increased with prolonged culture of hBMSCs. A greater percentage of hBMSCs lost their adipocyte differentiation potential in comparison to osteogenic differentiation potential during passaging [13]. There was an increase in osteogenesis at the basal level, coincident with decrease in cell proliferation with an increase in PD [17]. On the other hand, other groups have reported different results. Although human ASCs and rhesus BMSCs rapidly lost their osteogenic differentiation ability, they did not show decrease in chondrogenesis and adipogenesis, respectively [10]. The increase in clonogenicity and proliferative potential occurred with concurrent loss of multilineage differentiation potential in TDSCs with passaging in our study. This might be explained by the enrichment of stem/progenitor cells possessing less multilineage differentiation potential during subculture. Researchers and clinicians multiplying TDSCs in vitro for studying their roles in tendon physiology or pathology and potential applications of these cells in tissue engineering should consider the change in stem cell-related properties of these cells in vitro with prolonged subculture. With the increasing popularity and interest of using stem cells for tissue repair, the properties of stem cells should be thoroughly analyzed to ensure the safety and efficiency of their use in cell therapy and validity in basic research. Our results with rat TDSCs should be confirmed in the future with human cell studies.

The mechanisms of cellular senescence and reduction of multilineage differentiation potential of TDSCs in our study were not clear. The intrinsic transcriptional programs and the microenvironment/niche might control the decision of TDSCs to self-renew or differentiate [31]. Wnt proteins were reported to be important self-renewal factors for mammary gland stem cells [31]. Telomere shortening is suggested to be associated with cellular senescence [17,32]. Some studies reported the erosion of telomere during in vitro expansion of BMSCs [13,15,17,29,32]. In vitro culture of hBMSCs for just 7–10 PDs reduced the mean telomere restriction fragment length that was equivalent to the loss of more than half of their total replicative lifespan [17]. However, there were also papers reporting constant telomere length during in vitro passaging [10,12,33]. Whether MSCs have telomerase activity for counteracting the gradual loss of telomeres by de novo synthesis of telomere repeats is still a topic of debate. Some studies reported the presence [10,33–36], whereas others reported the absence of telomerase activity in BMSCs [15,17,29]. Izadpanah et al. [10] reported that MSCs from human and rhesus showed a marked decrease in telomerase activity over extended culture. However, there was no significant change in the mean telomere length up to 30 passages [10]. Such differences might arise from different cell types, culturing conditions, and sensitivity of different measuring methods.

One limitation of this study was that we used passage numbers instead of cumulative PD for studying the changes of stem cell-related properties of TDSCs during in vitro subculture. We counted the cell number and hence calculated the number of PDs of different passages of TDSCs when the cells reached 90% confluence. Cells at P5 reached 90% confluence at around day 5, whereas cells at P10, P20, and P30 reached 90% at around day 4 at the same initial seeding density (unpublished result). TDSCs at P5 replicated 3.3 ± 0.2 times in 5 days, whereas TDSCs at P10, P20, and P30 replicated 3.3 ± 0.1, 3.5 ± 0.1, and 3.4 ± 0.1 times in 4 days, respectively (mean ± standard deviation; unpublished result). On the basis of these data, we estimated that the cumulative PD of TDSCs at P5, P10, P20, and P30 to be around 17, 35, 70, and 105, respectively.

Conclusions

In conclusion, the senescence-associated β-galactosidase activity increased while the stem cell-related marker expression and the multilineage differentiation potential decreased in TDSCs with in vitro passaging. This occurred despite the increase in colony numbers and proliferative potential of TDSCs during subculture. Researchers and clinicians need to consider the changes of stem cell-related properties of TDSCs when multiplying them in vitro for tissue engineering.

Acknowledgments

This work was supported by equipment/resources donated by the Hong Kong Jockey Club Charities Trust and the CUHK Direct Grant (2009.1.043). This work was presented as a poster at the Proceedings of International Symposium of Ligament and Tendon (ISL&T) XI, January 12, 2011, Long Beach, California.

Author Disclosure Statement

No competing financial interests exist.

References

1. Lin TM, HW Chang, KH Wang, AP Kao, CC Chang, CH Wen, CS Lai and SD Lin. (2007). Isolation and identification of mesenchymal stem cells from human lipoma tissue. Biochem Biophys Res Commun 361:883–889.
2. Kim JW, SY Kim, SY Park, YM Kim, JM Kim, MH Lee and HM Ryu. (2004). Mesenchymal progenitor cells in the human umbilical cord. Ann Hematol 83:733–738.
3. Seo BM, M Miura, S Gronthos, PM Bartold, S Batouli, J Brahim, M Young, PG Robey and CY Wang. (2004). Investigation of multipotent postnatal stem cells from human periodontal ligament. Lancet 364:149–155.
4. Dowthwaite GP, JC Bishop, SN Redman, IM Khan, P Rooney, DJ Evans, L Haughton, Z Bayram, S Boyer, et al. (2004). The surface of articular cartilage contains a progenitor cell population. J Cell Sci 117(Pt. 6):889–897.
5. Qu-Petersen Z, B Deasy, R Jankowski, M Ikezawa, J Cummins, R Pruchnic, J Mytinger, B Cao, C Gates, A Wernig and J Huard. (2002). Identification of a novel population of muscle stem cells in mice: potential for muscle regeneration. J Cell Biol 157:851–864.
6. De Bari C, F Dell'Accio, J Vanlauwe, J Eyckmans, IM Khan, CW Archer, EA Jones, D McGonagle, TA Mitsiadis, C Pitzalis and FP Luyten. (2006). Mesenchymal multipotency of adult human periosteal cells demonstrated by single-cell lineage analysis. Arthritis Rheum 54:1209–1221.
7. De Bari C, F Dell'Accio, P Tylzanowski and FP Luyten. (2001). Multipotent mesenchymal stem cells from adult human synovial membrane. Arthritis Rheum 44:1928–1942.
8. Bi Y, D Ehirchiou, TM Kilts, TM Kilts, CA Inkson, MC Embree, W Sonoyama, L Li, AI Leet, et al. (2007). Identification of tendon stem/progenitor cells and the role of the extracellular matrix in their niche. Nat Med 13:1219–1227.

9. Rui YF, PPY Lui, G Li, SC Fu, YW Lee and KM Chan. (2010). Isolation and characterization of multi-potent rat tendon-derived stem cells. Tissue Eng Part A 16:1549–1558.
10. Izadpanah R, C Trygg, B Patel, C Kriedt, J Dufour, JM Gimble and BA Bunnell. (2006). Biologic properties of mesenchymal stem cells derived from bone marrow and adipose tissue. J Cell Biochem 99:1285–1297.
11. Izadpanah R, D Kaushal, C Kriedt, F Tsien, B Patel, J Dufour and BA Bunnell. (2008). Long-term *in vitro* expansion alters the biology of adult mesenchymal stem cells. Cancer Res 68:4229–4238.
12. Jiang Y, BN Jahagirdar, RL Reinhardt, RE Schwartz, CD Keene, XR Ortiz-Gonzalez, M Reyes, T Lenvik, T Lund, et al. (2002). Pluripotency of mesenchymal stem cells derived from adult marrow. Nature 418:41–49.
13. Bonab MM, K Alimoghaddam, F Talebian, SH Ghaffari, A Ghavamzadeh and B Nikbin. (2006). Aging of mesenchymal stem cell *in vitro*. BMC Cell Biol 7:14.
14. Muraglia A, R Cancedda and Quarto R. (2000). Clonal mesenchymal progenitors from human bone marrow differentiate *in vitro* according to a hierarchical model. J Cell Sci 113(Pt. 7):1161–1166.
15. Banfi A, A Muraglia, G Dozin, M Mastrogiacomo, R Cancedda and R Quarto. (2000). Proliferation kinetics and differentiation potential of *ex vivo* expanded human bone marrow stromal cells: implications for their use in cell therapy. Exp Hematol 28:707–715.
16. Bruder SP, N Jaiswal and SE Haynesworth. (1997). Growth kinetics, self-renewal, and the osteogenic potential of purified human mesenchymal stem cells during extensive subcultivation and following cryopreservation. J Cell Biochem 64:278–294.
17. Baxter MA, RF Wynn, SN Jowitt, JE Wraith, LJ Fairbairn and I Bellantuono. (2004). Study of telomere length reveals rapid aging of human marrow stromal cells following *in vitro* expansion. Stem Cells 22:675–682.
18. Rubio D, J Garcia-Castro, MC Martin, R de la Fuente, JC Cigudosa, AC Lloyd and A Bernad. (2005). Spontaneous human adult stem cell transformation. Cancer Res 65:3035–3039.
19. Miura Y, M Miura, S Gronthos, MR Allen, C Cao, TE Uveges, Y Bi, D Ehirchiou, A Kortesidis, S Shi and L Zhang. (2005). Defective osteogenesis of the stromal stem cells predisposes CD18-null mice to osteoporosis. Proc Natl Acad Sci USA 102:14022–14027.
20. Rui YF, PPY Lui, M Ni, LS Chan, YW Lee and KM Chan. (2011). Mechanical loading increased BMP-2 expression which promoted osteogenic differentiation of tendon-derived stem cells. J Orthop Res 29:390–396.
21. Conget PA and JJ Minguell. (1999). Phenotypical and functional properties of human bone marrow mesenchymal progenitor cells. J Cell Physiol 181:67–73.
22. Gregory CA, WG Gunn, A Peister and DJ Prockop. (2004). An Alizarin red-based assay of mineralization by adherent cells in culture: comparison with cetylpyridinium chloride extraction. Anal Biochem 329:77–84.
23. Lui PPY, LS Chan, YW Lee, SC Fu and KM Chan. (2010). Sustained expression of proteoglycans and collagen type III/type I ratio in a calcified tendinopathy model. Rheumatology 49:231–239.
24. Zhang J and JHC Wang. (2010). Characterization of differential properties of rabbit tendon stem cells and tenocytes. BMC Musculoskelet Disord 11:10.
25. Halfon S, N Abramov, B Grinblat and I Ginis. (2011). Markers distinguishing mesenchymal stem cells from fibroblasts are downregulated with passaging. Stem Cells Dev 20: 53–66.
26. Mitchell JB, K McIntosh, S Zvonic, S Garrett, ZE Floyd, A Kloster, Y Di Halvorsen, RW Storms, B Goh, et al. (2006). Immunophenotype of human adipose-derived cells: temporal changes in stromal-associated and stem cell-associated markers. Stem Cells 24:376–385.
27. Digirolamo CM, D Stokes, D Colter, DG Phinney, R Class and DJ Prockop. (1999). Propagation and senescence of human marrow stromal cells in culture: a simple colony-forming assay identifies samples with the greatest potential to propagate and differentaite. Br J Haematol 107:275–281.
28. Sugiura F, H Kitoh and N Ishiguro. (2004). Osteogenic potential of rat mesenchymal stem cells after several passages. Biochem Biophys Res Commun 316:233–239.
29. Stenderup K, J Justesen, C Clausen and M Kassem. (2003). Aging is associated with decreased maximal life span and accelerated senescence of bone marrow stromal cells. Bone 33:919–926.
30. Rombouts WJ and RE Ploemacher. (2003). Primary murine MSC show highly efficient homing to the bone marrow but lose homing ability following culture. Leukemia 17:160–170.
31. Zeng YA and R Nusse. (2010). Wnt proteins are self-renewal factors for mammary stem cells and promote their long-term expansion in culture. Cell Stem Cell 6:568–577.
32. Parsch D, J Fellenberg, TH Brummdorf, AM Eschlbeck and W Richter. (2004). Telomere length and telomerase activity during expansion and differentiation of human mesenchymal stem cells and chondrocytes. J Mol Med 82:49–55.
33. Lee JJ, CE Nam, H Kook, JP Maciejewski, YK Kim, IJ Chung, KS Park, IK Lee, TJ Hwang and HJ Kim. (2003). Constitution and telomere dynamics of bone marrow stromal cells in patients undergoing allogeneic bone marrow transplantation. Bone Marrow Transplant 32:947–952.
34. Seruya M, A Shah, D Pedrotty, T du Laney, R Melgiri, JA McKee, HE Young and LE Niklason. (2004). Clonal population of adult stem cells: life span and differentiation potential. Cell Transplant 13:93–101.
35. Yoon YS, A Wecker, L Heyd, JS Park, T Tkebuchava, K Kusano, A Hanley, H Scadova, G Qin, et al. (2005). Clonally expanded novel multipotent stem cells from human bone marrow regenerate myocardium after myocardial infarction. J Clin Invest 115:326–338.
36. Pittenger MF, AM Mackay, SC Beck, RK Jaiswal, R Douglas, JD Mosca, MA Moorman, DW Simonetti, S Craig and DR Marshak. (1999). Multilineage potential of adult human mesenchymal stem cells. Science 284:143–147.

Address correspondence to:
Prof. Pauline Po Yee Lui
Department of Orthopaedics and Traumatology
The Chinese University of Hong Kong
Prince of Wales Hospital
Room No. 74025, 5/F, Clinical Sciences Building
Shatin
Hong Kong SAR
China

E-mail: pauline@ort.cuhk.edu.hk

Received for publication April 1, 2011
Accepted after revision May 31, 2011
Prepublished on Liebert Instant Online June 1, 2011